Mineralogical Magazine, April 2011, Vol. 75(2), pp. 363–374

Thermal expansion of andalusite and sillimanite at ambient pressure: a powder X-ray diffraction study up to 1000ºC

X. HU[1,2], X. LIU[1,2,*], Q. HE[1,2], H. WANG[1,2], S. QIN[1,2], L. REN[3], C. M. WU[4] AND L. CHANG[1,2]

[1] The Key Laboratory of Orogenic Belts and Crustal Evolution, Ministry of Education of China, Beijing 100871, China
[2] School of Earth and Space Sciences, Peking University, Beijing 100871, China
[3] Institute of Geology, Chinese Academy of Geological Sciences, Beijing 100037, China
[4] College of Earth Science, the Graduate School, Chinese Academy of Sciences, Beijing 100049, China

[*Received 16 February 2011; Accepted 18 March 2011*]

ABSTRACT

The unit-cell parameters of andalusite and sillimanite have been measured by high-T powder X-ray diffraction up to 1000ºC at ambient pressure. Within the temperature range investigated, all the unit-cell parameters varied smoothly, indicating no phase transition. The volume-temperature data were fitted with a polynomial expression for the thermal expansion coefficient ($\alpha_T = a_0 + a_1T + a_2T^{-2}$), yielding $a_0 = 2.55(2) \times 10^{-5}K^{-1}$, $a_1 = 0$ and $a_2 = 0$ for andalusite, and $a_0 = 1.40(4) \times 10^{-5}K^{-1}$, $a_1 = 7.1(8) \times 10^{-9}K^{-2}$ and $a_2 = 0$ for sillimanite. Using the new thermal expansion data determined in the present study and compressional data from the literature, the P-T phase relations of the kyanite-andalusite-sillimanite system were calculated thermodynamically, with the invariant point located at ~523ºC and 3.93 kbar.

KEYWORDS: andalusite, high temperature, powder X-ray diffraction, sillimanite, thermal expansion.

Introduction

THE aluminium silicate polymorphs: kyanite (Ky), andalusite (And) and sillimanite (Sil) (Al_2SiO_5) are common metamorphic minerals in metapelites, and their P-T phase relations have important applications in metamorphic thermobarometry and petrology (Kerrick, 1990, and references therein). Many high-P experimental investigations and thermodynamic analyses have been carried out in the Ky-And-Sil system. Despite all these efforts, however, the phase relations of the Ky-And-Sil system remain poorly constrained experimentally, mainly due to the very slow polymorphic phase transition rate in the high-P experiments. The phase relations of this system, generally accepted nowadays, are that: (1) the invariant point of Ky + And + Sil is located at ~4.3 kbar and 550ºC (figure 3.46 of Kerrick, 1990); (2) And is stable at relatively low P-T conditions, Sil is stable at relatively low P but high T conditions, and Ky is stable at relatively high P but low T conditions; (3) at low P and very high T, Sil breaks down to mullite + tridymite (Beger, 1979); (4) at pressures of ~16 GPa, Ky breaks down to stishovite + corundum (Liu, 1974; Irifune *et al*., 1995; Schmidt *et al*., 1997; Liu *et al*., 2006; Ono *et al*., 2007).

Accurate derivation of the Al_2SiO_5 phase relations through measurements of the thermodynamic properties is an alternative to the method of high-P experimentation. Due to the small Gibbs free energy change along the polymorphic phase transitions, however, relatively small errors in the enthalpies, entropies, and volumes of the phases lead to significant errors in the P-T location of the univariant curves. Therefore, accurate volume data at high pressures and high temperatures are desirable.

* E-mail: xi.liu@pku.edu.cn
DOI: 10.1180/minmag.2011.075.2.363

The compressibility of Ky has been investigated both by high-*P* experiments (Brace *et al*., 1969; Comodi *et al*., 1997; Yang *et al*., 1997*a*; Friedrich *et al*., 2004; Liu *et al*., 2009) and by theoretical simulations (Matsui, 1996; Oganov and Brodholt, 2000; Winkler *et al*., 2001). As summarized by Liu *et al*. (2009), the bulk modulus and its pressure derivative of Ky at ambient temperature have been well established, and are close to 196(6) GPa and 4, respectively. The thermal expansion of Ky at high temperatures has been investigated in four experimental studies (Skinner *et al*., 1961; Winter and Ghose, 1979; Gatta *et al*., 2006; Liu *et al*., 2010). Despite some scattering in the variation of the unit-cell parameters α, β and γ with temperature, the values of the axial and volumetric thermal expansion coefficients of Ky determined in these different experimental investigations with different experimental techniques show a good consistency (Winter and Ghose, 1979; Gatta *et al*., 2006; Liu *et al*., 2010).

The compressibility of And and Sil has been investigated by high-*P* experimentation and theoretical calculation, and good agreement has been obtained. In the case of And, the experimental studies include Brace *et al*. (1969), Vaughan and Weidner (1978), Ralph *et al*. (1984) and Burt *et al*. (2006) whereas the theoretical studies include Matsui (1996), Oganov and Brodholt (2000) and Winkler *et al*. (2001); the bulk modulus of And and its pressure derivative are 144.2(7) GPa and 6.8(2), respectively, according to the most recent experimental determination (Burt *et al*., 2006). In the case of Sil, the experimental studies include Brace *et al*. (1969), Vaughan and Weidner (1978), Yang *et al*. (1997*b*), Friedrich *et al*. (2004) and Burt *et al*. (2006) whereas the theoretical studies include Matsui (1996), Oganov and Brodholt (2000) and Winkler *et al*. (2001); the bulk modulus of Sil and its pressure derivative are 164(1) GPa and 5.0(3), respectively, according to Burt *et al*. (2006). In contrast, the thermal expansion of And and Sil has been much less studied. For both And and Sil there have been only two detailed experimental investigations published so far (Skinner *et al*., 1961; Winter and Ghose, 1979), and the derived volumetric thermal expansion coefficients are, unfortunately, in apparent disagreement (Liu *et al*., 2010).

Because of this, a further investigation of the thermal expansion of And and Sil is required and is the aim of the present study.

Materials characterization and high-*T* experimental details

The gem-quality prismatic crystal of And used in this study is from the famous andalusite deposit in Xixia, Henan province, P.R. China, which is hosted by quartz schist (Zhou and Feng, 1999). Part of the crystal was mounted in epoxy, polished using a series of diamond pastes, cleaned using an ultrasonic washing machine, carbon-coated and examined with a JEOL 8100 electron microprobe at the School of Earth and Space Sciences, Peking University. The operating conditions of the electron microprobe were 15 kV, 10 nA specimen current, and 40 s counting time per analysis. The electron microprobe analyses (EMPA) reveal that the And contains a negligible amount of Fe_2O_3 (~0.2 wt.%, with all Fe assumed as Fe^{3+}), and its chemical formula is essentially Al_2SiO_5 (10 EMPA analyses). According to Zhou and Feng (1999), the minerals coexisting with the And from the andalusite deposit in Xixia are quartz, biotite, K-feldspar, muscovite, garnet, staurolite, magnetite and pyrite. Around part of the crystal edge of our And sample, minerals such as K-feldspar ($Or_{99}Ab_1$; four EMPA analyses), ilmenite ($(Si_{0.005}Al_{0.003}Mn_{0.049}Fe_{0.906}Ti_{1.015})O_3$; three EMPA analyses), biotite ($(K_{2.07}Na_{0.057}Ca_{0.001})(Mg_{1.893}Mn_{0.014}Fe_{2.542}Ti_{0.163}Al_{0.972})(Al_{2.615}Si_{5.385})O_{22}$ with volatile components ignored; four EMPA analyses), muscovite ($(K_{1.681}Na_{0.269}Ca_{0.029})(Mg_{0.068}Mn_{0.001}Fe_{0.120}Ti_{0.020}Al_{3.823})(Al_{1.945}Si_{6.055})O_{22}$ with volatile components ignored; four EMPA analyses) and quartz were detected. Part of the clean And crystal was finely crushed under acetone and used as one of the starting materials in our high-*T* powder X-ray diffraction (XRD) experiments.

The other starting material used in our high-*T* powder XRD experiments, sillimanite, is from the high-grade quartzofeldspathic gneisses in the Larsemann Hills, East Antarctica (Ren *et al*., 2007, 2009). Some prismatic Sil crystals, up to 2 cm long, were hand-picked from the disaggregated rock chips, cleaned twice in 2.4 N hydrochloric acid and rinsed thoroughly in deionized water with the aid of an ultrasonic washing machine. Unfortunately, the vibration of the ultrasonic wave broke the Sil crystals into pieces so we were forced to use the bulk material in order to proceed. This bulk material was ground thoroughly under acetone. The X-ray data revealed that it contained a significant amount of low-quartz, which we were able to use as an

internal standard in our experiments. Some other crystals, hand-picked from the disaggregated rock chips, were mounted in epoxy and processed for later EMPA analyses. The EMPA analyses revealed that the Sil crystals contain ~1.2 wt.% Fe_2O_3, and its chemical formula is $(Al_{1.977}Fe_{0.028})Si_{0.995}O_5$. Along the edge of one Sil crystal, two Fe-rich minerals were found, and they are probably magnetite and hematite, according to our EMPA analyses and to Ren *et al*. (2009). Therefore, the Sil sample used in this study is similar to the material from the Benson Mines, New York, which contains identical amounts of iron and coexists with magnetite and hematite (Todd, 1950; Skinner *et al*., 1961).

Both materials were characterized at room *T* and room *P* using the powder X-ray diffractometer hosted at the School of Earth and Space Sciences, Peking University (X'Pert Pro MPD system; Cu-$K\alpha_1$ X-ray radiation): the And material contained andalusite only, and its XRD pattern was identical to that of the JCPDS reference pattern card 13-122; on the other hand, the Sil material contained both sillimanite and low-quartz, in reference to the JCPDS reference cards 22-18 and 46-1045, respectively.

The X'Pert Pro MPD system at the School of Earth and Space Sciences, Peking University, was also used in our high-*T* XRD experiments at ambient pressure. An attached Anton Paar HTK-1200N oven running with a Eurotherm temperature controller (Eurotherm 2604; type S thermocouple) was employed to heat the sample (~0.20−0.25 g in weight). The maximum temperature achievable with this heating system is 1200ºC with an accuracy of ±2ºC; the controlling thermocouple was checked against the melting point of NaCl. In order to protect the heating element, the oven was run in a vacuum chamber with a nickel window. The X'Pert Pro MPD diffractometer system was equipped with a Cu target, and was operated at 40 kV, 40 mA, and with a scanning step length of 0.017º2θ in our experiments. The alignment was achieved with a standard of silicon crystalline powder at ambient temperature only; in addition, the small amount of quartz impurity in our Sil sample served as an internal standard, providing additional evaluation on the quality of the X-ray data collected at high temperatures.

High-*T* experiments for both samples were conducted up to 1000ºC, and the heating and data-collection procedures were as follows: after collection of the XRD data at a given temperature, the sample was heated to the next setpoint at a rate of 10ºC/min and then allowed to relax for 5 min before collection of the powder diffraction spectrum. X-ray data were collected between 10 and 80º2θ.

Following the above-mentioned experimental procedures, realignment of the experimental system was apparently not made at high temperatures. Due to the thermal expansion of the furnace and sample holder components, the sample position was changed slightly as temperature increased, so that the XRD data were affected by the small sample displacement. In order to correct for this effect, we processed the X-ray data using the MDI program *Jade* 5.0 (Material Data, Inc.). With a full powder XRD pattern refinement, the influence of the sample displacement was corrected and accurate unit-cell parameters were refined automatically by the software.

Results and discussion

High-*T* experiments for both And and Sil were conducted up to 1000ºC at ambient pressure, and no evidence of phase transition was observed, in agreement with previous high-temperature investigations (Skinner *et al*., 1961; Winter and Ghose, 1979). Typical powder XRD patterns are shown in Fig. 1, and the unit-cell parameters derived at different temperatures are listed in Table 1. On the other hand, the small amount of quartz impurity in the Sil material underwent a low-quartz–high-quartz phase transition at high temperature. As shown in Fig. 2, the thermal behaviour of low-quartz and high-quartz follows closely the trend determined by Carpenter *et al.* (1998), suggesting that our data-processing protocol was successful.

Figure 3 shows the unit-cell parameters of And with temperature: with the exception of the *b* axis, the correlations between other unit-cell parameters and temperature are almost linear. Although this study and that by Skinner *et al*. (1961) used similar experimental techniques (powder XRD), the agreement between the two investigations is generally poor (Fig. 3*b*−*d*), especially in the case of the *c* axis and the volume. The lengths of the *c* axes of And in Skinner *et al*. (1961) was calculated directly by using peaks 002 and 004 only, which unfortunately overlapped with peaks 220 and 440, respectively (Fig. 1*a*). The lengths of the *a* and *b* axes of And in Skinner *et al*. (1961) were

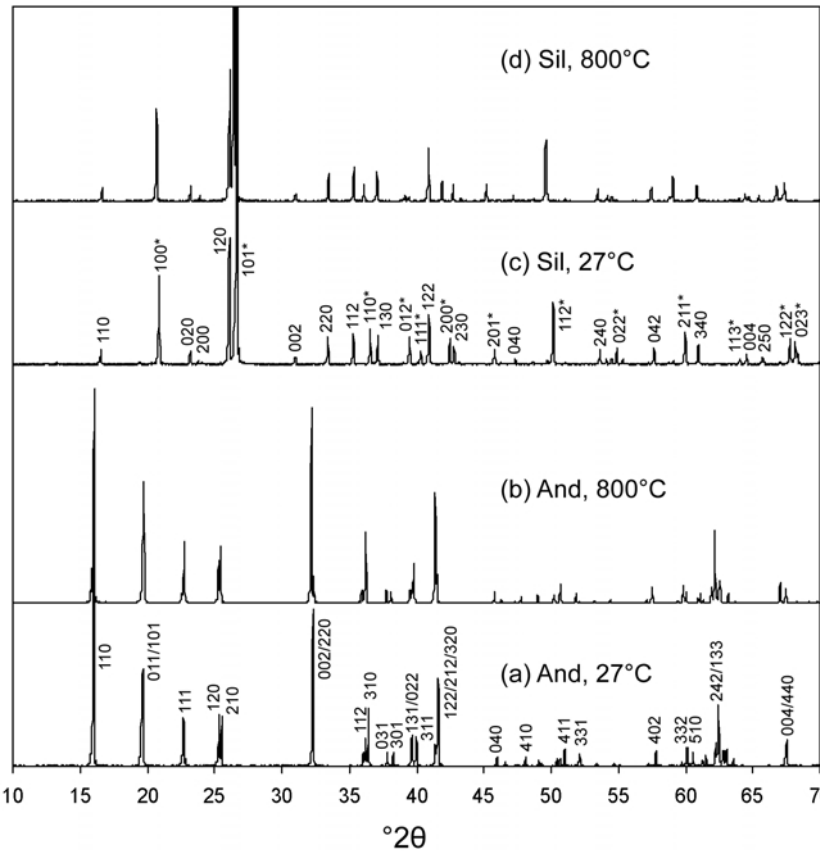

FIG. 1. XRD patterns of And and Sil at ambient temperature and 800ºC. The Bragg peaks of quartz in the Sil sample are denoted by asterisks.

calculated by using the free-standing peaks 301 and 031, so that they were relatively less problematic. The large errors in the lengths of the *c* axes severely influenced the volume data of And in Skinner *et al*. (1961). In comparison, our results show good agreement with those of Winter and Ghose (1979).

Figure 4 shows the unit-cell parameters of Sil with temperature. For all three axial dimensions, the average slopes of the curves defined by our data fall between those constrained by Skinner *et al*. (1961) and Winter and Ghose (1979). Although no detailed chemical analyses were available, the Sil samples used by Skinner *et al*. (1961; Williamstown, South Australia) and Winter and Ghose (1979; Brandywine Springs, Delaware) were probably Fe-free (Skinner *et al*., 1961), so that the compositional difference of the Sil samples used in this study and in the previous two studies could explain some of the difference in the experimental results. As indicated by Fig. 4, the axial thermal expansion obtained by Skinner *et al*. (1961) is significantly larger than that obtained in the present this study and by Winter and Ghose (1979).

Figure 5 shows the variation of the *a*/*c* and *b*/*c* ratios of And and Sill with temperature, suggesting that both minerals are elastically anisotropic. As temperature increases, both the *a*/*c* and *b*/*c* ratios of And increase, but the rates are different (Fig. 5*a*): from 27 to 1000ºC, the *a*/*c* ratio increases by ~1% (from 1.4033(1) to 1.4173(1)) whereas the *b*/*c* ratio increases by ~0.65% only (from 1.4220(1) to 1.4313(1)). It follows that the *a* axis is thermally more expandable than the *b* axis, which is in turn more expandable than the *c* axis. These findings are in good agreement with the Brillouin scattering measurements made by Vaughan and Weidner (1978). In the case of Sil (Fig. 5*b*), the

TABLE 1. Unit-cell parameters of andalusite and sillimanite at various temperatures. Standard deviations are in parentheses.

T (ºC)	*a* (Å)	*b* (Å)	*c* (Å)	*V* (Å^3)	*a*/*c*	*b*/*c*
Andalusite						
27	7.7944(2)	7.8981(3)	5.5542(4)	341.92(3)	1.4033(1)	1.4220(1)
50	7.7967(3)	7.9003(3)	5.5546(5)	342.14(4)	1.4037(1)	1.4223(1)
100	7.8007(3)	7.9023(4)	5.5554(5)	342.45(4)	1.4042(1)	1.4225(1)
150	7.8068(2)	7.9065(2)	5.5559(3)	342.94(2)	1.4051(1)	1.4231(1)
200	7.8106(3)	7.9089(3)	5.5570(4)	343.27(3)	1.4056(1)	1.4232(1)
250	7.8157(3)	7.9128(3)	5.5577(4)	343.71(3)	1.4063(1)	1.4238(1)
300	7.8222(3)	7.9178(3)	5.5587(5)	344.27(3)	1.4072(1)	1.4244(1)
350	7.8267(2)	7.9215(3)	5.5591(3)	344.66(3)	1.4079(1)	1.4250(1)
400	7.8311(3)	7.9241(3)	5.5595(3)	344.99(2)	1.4086(1)	1.4253(1)
450	7.8362(3)	7.9291(4)	5.5612(5)	345.54(4)	1.4091(1)	1.4258(1)
500	7.8413(4)	7.9317(3)	5.5611(4)	345.87(3)	1.4100(1)	1.4263(1)
550	7.8483(3)	7.9377(3)	5.5627(4)	346.55(3)	1.4109(1)	1.4269(1)
600	7.8517(3)	7.9392(3)	5.5627(3)	346.75(3)	1.4115(1)	1.4272(1)
650	7.8568(3)	7.9440(3)	5.5635(4)	347.24(3)	1.4122(1)	1.4279(1)
700	7.8640(3)	7.9481(2)	5.5650(3)	347.83(3)	1.4131(1)	1.4282(1)
750	7.8669(4)	7.9524(4)	5.5652(6)	348.16(5)	1.4136(1)	1.4290(1)
800	7.8727(3)	7.9551(3)	5.5663(3)	348.60(3)	1.4144(1)	1.4292(1)
850	7.8759(4)	7.9596(5)	5.5674(6)	349.01(5)	1.4146(1)	1.4297(1)
900	7.8834(4)	7.9636(3)	5.5681(3)	349.57(3)	1.4158(1)	1.4302(1)
950	7.8886(6)	7.9700(5)	5.5686(6)	350.11(5)	1.4166(1)	1.4312(1)
1000	7.8941(5)	7.9721(4)	5.5699(4)	350.53(3)	1.4173(1)	1.4313(1)
Sillimanite						
27	7.4900(3)	7.6777(1)	5.7753(2)	332.11(2)	1.2969(1)	1.3294(1)
50	7.4902(4)	7.6792(2)	5.7762(2)	332.24(2)	1.2967(1)	1.3295(1)
100	7.4905(4)	7.6817(2)	5.7780(2)	332.46(2)	1.2964(1)	1.3295(1)
150	7.4911(5)	7.6844(2)	5.7787(3)	332.65(3)	1.2963(1)	1.3298(1)
200	7.4922(4)	7.6875(2)	5.7795(2)	332.88(2)	1.2964(1)	1.3301(1)
250	7.4932(4)	7.6908(1)	5.7810(2)	333.15(2)	1.2962(1)	1.3304(1)
300	7.4939(4)	7.6941(1)	5.7827(2)	333.43(2)	1.2959(1)	1.3305(1)
350	7.4948(4)	7.6973(2)	5.7840(2)	333.68(2)	1.2958(1)	1.3308(1)
400	7.4958(4)	7.7005(2)	5.7853(2)	333.93(2)	1.2957(1)	1.3310(1)
450	7.4968(3)	7.7039(1)	5.7870(2)	334.22(2)	1.2955(1)	1.3312(1)
500	7.4984(4)	7.7079(1)	5.7889(2)	334.58(2)	1.2953(1)	1.3315(1)
550	7.5005(4)	7.7114(1)	5.7906(2)	334.92(2)	1.2953(1)	1.3317(1)
600	7.5020(4)	7.7153(2)	5.7921(2)	335.25(2)	1.2952(1)	1.3320(1)
650	7.5030(4)	7.7192(2)	5.7942(3)	335.58(3)	1.2949(1)	1.3322(1)
700	7.5040(3)	7.7218(2)	5.7952(3)	335.80(2)	1.2949(1)	1.3324(1)
750	7.5050(3)	7.7256(2)	5.7970(2)	336.12(2)	1.2946(1)	1.3327(1)
800	7.5060(3)	7.7297(1)	5.7991(2)	336.46(2)	1.2943(1)	1.3229(1)
850	7.5067(4)	7.7334(2)	5.8011(2)	336.77(2)	1.2940(1)	1.3331(1)
900	7.5090(4)	7.7374(2)	5.8027(2)	337.14(3)	1.2940(1)	1.3334(1)
950	7.5102(4)	7.7407(2)	5.8041(2)	337.42(2)	1.2939(1)	1.3337(1)
1000	7.5119(4)	7.7445(2)	5.8062(1)	337.78(2)	1.2938(1)	1.3338(1)

b/*c* ratio increases whereas the *a*/*c* ratio decreases with *T*: from 27 to 1000ºC, the *a*/*c* ratio decreases by ~0.24% (from 1.2969(1) to 1.2938(1)) whereas the *b*/*c* ratio increases by ~0.33% (from 1.3294(1) to 1.3338(1)). According to Winter and Ghose (1979), the different variation patterns of the *a*/*c* and *b*/*c* ratios with *T* are related to the rotation mechanism of the relatively rigid [$Al2O_4$] and [SiO_4] tetrahedra (labelling follows that in Yang *et al*. (1997*b*)): with increasing temperature, one

tetrahedron rotates clockwise while the other rotates anticlockwise, so that the expansion along the *b* axis is enhanced whereas that along the *a* axis is suppressed. Combining the *a*/*c* ratio with the *b*/*c* ratio of Sil, we find that the *b* axis is thermally more expandable than the *c* axis, which, in turn, is more expandable than the *a* axis. This is also in good agreement with the Brillouin scattering measurements made by Vaughan and Weidner (1978).

In general, temperature and pressure have opposite effects on changes in the crystal structures of many silicate minerals (Hazen and Finger, 1982). For the Al silicates, however, the opposite effects of temperature and pressure do not always hold strictly (Ralph *et al*., 1984; Yang *et al*., 1997*b*). Recently Liu *et al*. (2010) showed that the *c* axis of Ky has the largest compressibility and thermal expansibility, the *a* axis has the smallest compressibility and thermal expansibility, and the opposite effects are generally identical in magnitude. However, kyanite is triclinic, so that

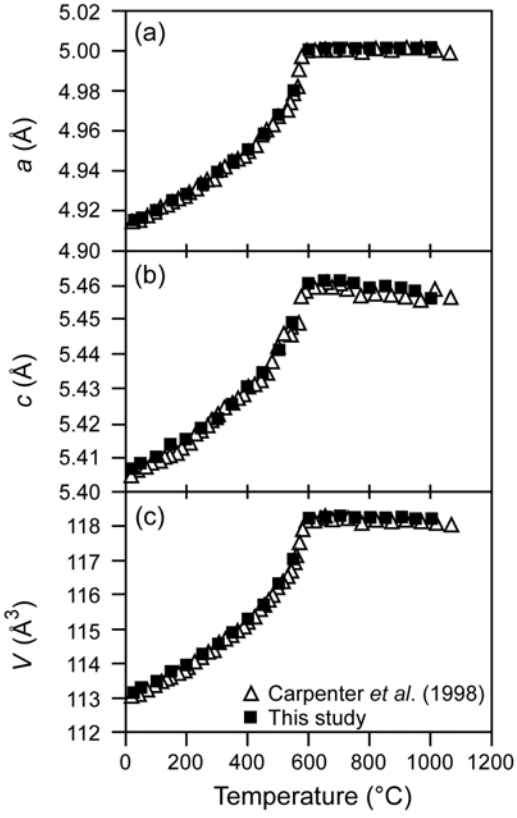

FIG. 2. Variation of the unit-cell parameters of quartz with temperature: (*a*) the *a* axis; (*b*) the *c* axis; (*c*) the volume.

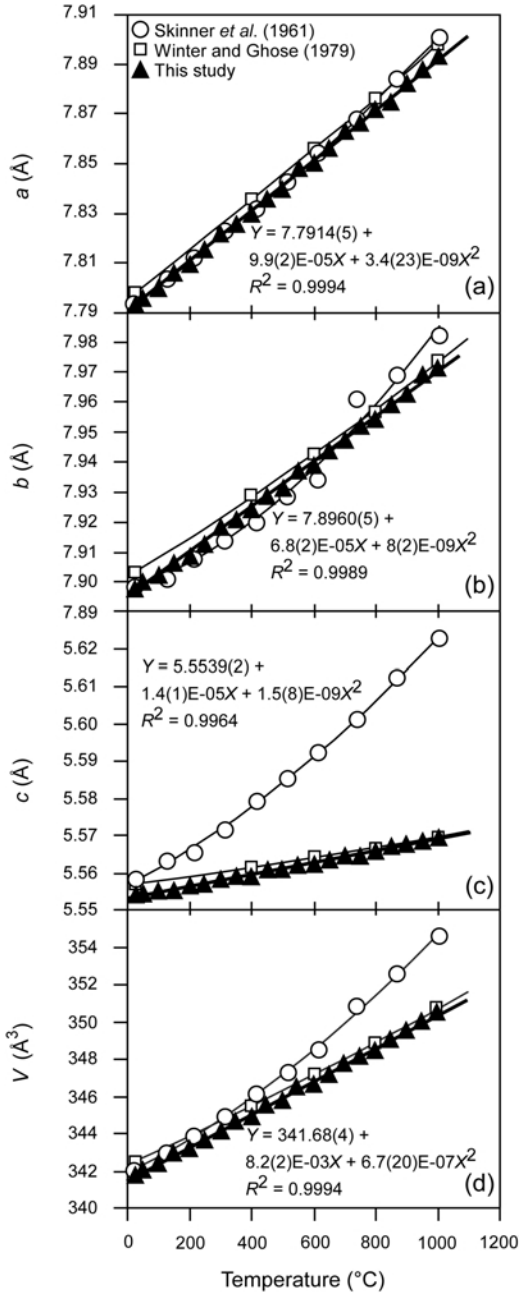

FIG. 3. Variation of the unit-cell parameters of And with temperature. The equations shown are regressed from the experimental data collected in this investigation. For all data the error bars are smaller than the symbol sizes.

the principal axes of its strain ellipsoid do not necessarily coincide with its unit-cell axes. Here we show the effects of isobaric thermal expansion and isothermal compression on modifying the crystal structures of And and Sil (Fig. 6). In Fig. 6*a* the magnitude of the effect of pressure on the three axes of And is seen to decrease in the order of the *a* axis, *b* axis and *c* axis, in parallel to that of the effect of temperature. Although the data points for the *a* and *b* axes both at ambient *P*-high *T* and at ambient *T*-high *P* fall on almost straight lines; the data points for the *c* axis do not, confirming the observation made by Ralph *et al*. (1984). In the case of Sil, only the datum points for the *b* axis fall on an almost straight line. Moreover, the order of the magnitude of the effect of pressure on the three axes is not identical to that of the magnitude of the effect of temperature (Fig. 6*b*): at ambient *P*-high *T*, it decreases from the *b* axis, *c* axis to *a* axis while it decreases from the *b* axis, *a* axis to *c* axis at ambient *T*-high *P*, as observed by Yang *et al*. (1997*b*). It follows that the crystal structure plays an important role in the microstructure response to the change of pressure and temperature.

The volume-temperature data of And and Sil have been fitted to the following equations:

$$V_T = V_0 \exp\left[\int_0^T \alpha_T dT\right]$$

and

$$\alpha_T = a_0 + a_1 T + a_2 T^{-2}$$

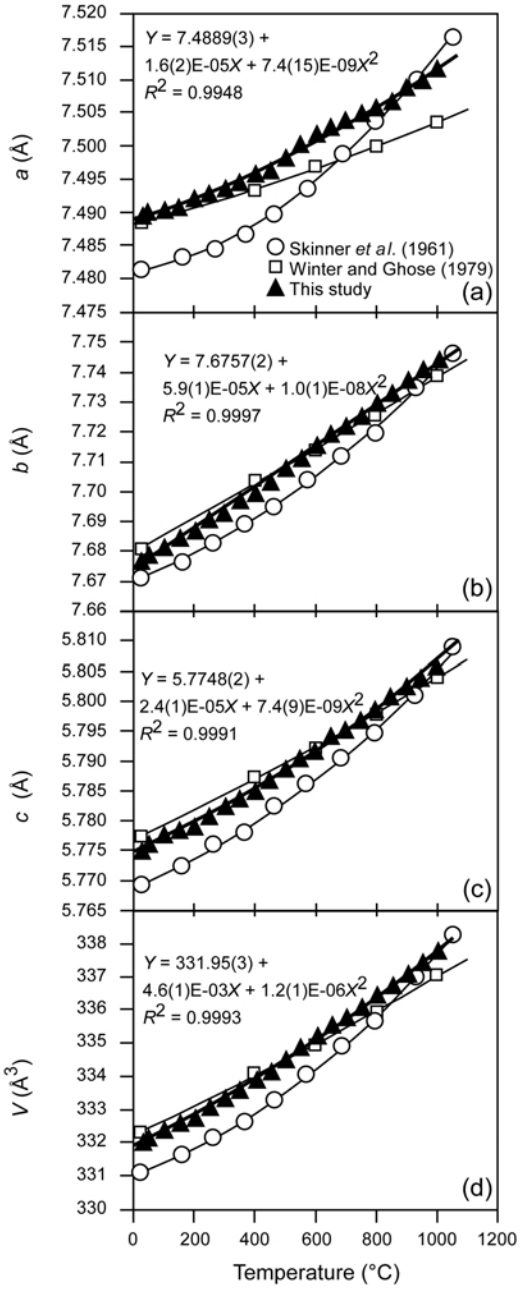

FIG. 4. Variation of the unit-cell parameters of Sil with temperature. The equations shown are regressed from the experimental data collected in this investigation. For all data the error bars are smaller than the symbol sizes.

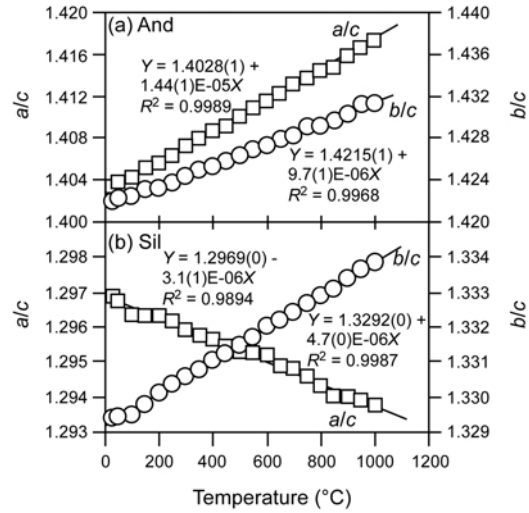

FIG. 5. Variation of the *a*/*c* and *b*/*c* ratios of And and Sil with temperature. For all data the error bars are smaller than the symbol sizes.

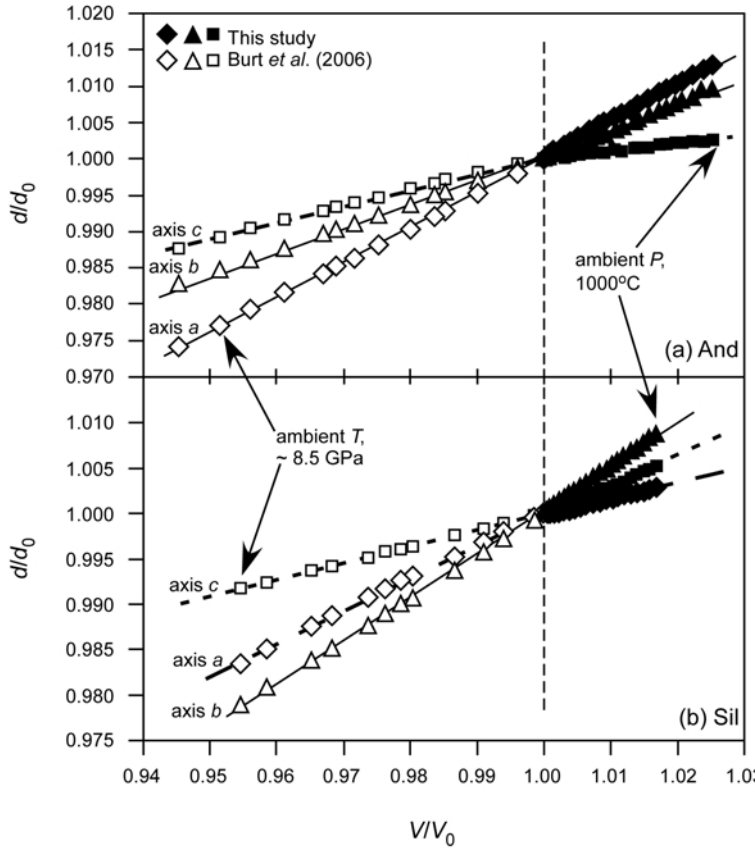

FIG. 6. Variation of unit-cell dimensions (d/d_0) with V/V_0: (*a*) And, (*b*) Sil. Solid symbols represent the thermal expansion data at ambient *P* whereas open symbols represent the compression data at ambient *T*. Lines are drawn to guide the eye.

where V_T and V_0 are the volume at high temperature, *T*, and room temperature, respectively, α_T is the volumetric thermal expansion coefficient at temperature *T*, and a_0, a_1 and a_2 are constants determined by fitting the experimental *V*-*T* data. Replacing the volume data in the equations above with the axial data, the axial thermal expansion coefficients can be obtained similarly. Table 2 lists all the derived axial and volumetric thermal expansion coefficients of And and Sil. For comparison, the volume-temperature data of kyanite from the literature have also been processed using the same procedure, and the thermal expansion coefficients derived are listed in Table 2. Clearly, the order of the volumetric thermal expansivity of these three minerals is And > Ky > Sil. In contrast, the order of the volumetric compressibility is Ky > Sil > And (Yang *et al*., 1997*a*,*b*; Burt *et al*., 2006; Liu *et al*., 2009).

With the most recent compression and thermal expansion data of Ky, And and Sil (Burt *et al*., 2006; Liu *et al*., 2009; Liu *et al*., 2010; this study), along with other thermodynamic data for these three minerals from Robie and Hemingway (1995), we used the following equations to calculate the univariant curves in the Ky-And-Sil system:

$$\Delta G_{r(T,P)} = \Delta G^0_{r(T,1\mathrm{bar})} + \int_1^P \Delta V_T(P)dP + \mathrm{R}T\ln K = 0$$

and

$$\Delta G^0_{r(T,1\ \mathrm{bar})} = \Delta H^0_{r(T)} - T\Delta S^0_{r(T)}$$

where $\Delta G_{r(T,P)}$ is the Gibbs free energy change for the reaction at the pressure and temperature of

TABLE 2. Thermal expansion coefficients ($\alpha_T = a_0 + a_1T + a_2T^{-2}$) of andalusite, sillimanite and kyanite. Standard deviations are in parentheses.

Data source		*a*	*b*	*c*	*V*
Andalusite					
This study	$a_0(10^{-6})$	13.0(1)	8.6(3)	2.8(0)	25.5(2)
	$a_1(10^{-9})$	–	2.0(6)	–	–
	a_2	–	–	–	–
Skinner *et al.*	$a_0(10^{-6})$	11.2(2)	5.0(17)	8.1(5)	24.3(18)
(1961)	$a_1(10^{-9})$	4.8(4)	12.1(33)	7.5(9)	24.5(36)
	a_2	–	–	–	–
Winter and Ghose	$a_0(10^{-6})$	12.5(2)	8.0(5)	2.4(1)	24.3(4)
(1979)	$a_1(10^{-9})$	1.0(4)	2.0(9)	–	–
	a_2	–	–	–	–
Sillimanite					
This study	$a_0(10^{-6})$	2.1(2)	7.7(2)	4.2(2)	14.0(4)
	$a_1(10^{-9})$	2.0(4)	2.6(3)	2.5(3)	7.1(8)
	a_2	–	–	–	–
Skinner *et al.*	$a_0(10^{-6})$	1.1(2)	5.2(3)	3.6(4)	9.9(4)
(1961)	$a_1(10^{-9})$	6.5(4)	8.0(6)	5.4(7)	19.9(8)
	a_2	–	–	–	–
Winter and Ghose	$a_0(10^{-6})$	2.1(1)	3.9(3)	2.8(2)	8.8(2)
(1979)	$a_1(10^{-9})$	–	5.2(4)	2.9(3)	8.2(3)
	a_2	–	0.0142(13)	0.0055(9)	0.0179(8)
Kyanite					
Liu *et al.*	$a_0(10^{-6})$	8.4(4)	7.6(2)	9.4(2)	20.3(16)
(2010)	$a_1(10^{-9})$	–	–	–	10.1(31)
	a_2	–	–	–	–
Skinner *et al.*	$a_0(10^{-6})$	9.6(3)	6.9(2)	10.7(3)	27.8(7)
(1961)	$a_1(10^{-9})$	–	2.9(3)	–	–
	a_2	–	–	–	–
Winter and Ghose	$a_0(10^{-6})$	7.8(7)	7.3(2)	10.7(5)	25.0(7)
(1979)	$a_1(10^{-9})$	–	−1.9(4)	–	–
	a_2	–	–	–	–
Gatta *et al.*	$a_0(10^{-6})$	7.5(2)	7.4(2)	9.4(1)	24.8(3)
(2006)	$a_1(10^{-9})$	–	–	–	–
	a_2	–	–	–	–

interest, $\Delta G^0_{r(T,1\,\mathrm{bar})}$ is the Gibbs free energy change for the reaction at 1 bar and the temperature of interest, $\Delta V_T(P)$ is the volume change for the reaction at the pressure and temperature of interest calculated readily from the expansivity and compressibility of the minerals, P is the pressure, R is the universal gas constant (8.3143 J K^{-1} mol^{-1}), T is the temperature, and $K = 1$ for the Ky-And-Sil system. The result is plotted in Fig. 7, which shows the invariant point of Ky + And + Sil at ~523ºC and 3.93 kbar (the slope of the Ky-And univariant curve is ~11.3 bar/K, that of the Ky-Sil univariant curve is 20.6 bar/K and that of the And-Sil univariant curve is −16.8 bar/K). In comparison, the thermodynamic analysis by Berman (1988) placed the invariant point at ~506ºC and 3.73 kbar while that by Holland and Powell (1985) positioned the invariant point at ~560ºC and 4.5 kbar. Kerrick (1990) carried out a critical evaluation of early experimental studies and thermodynamic analyses in the Ky-And-Sil system, and placed the invariant point at 550ºC and 4.3 kbar (Fig. 7). On the other hand, the most

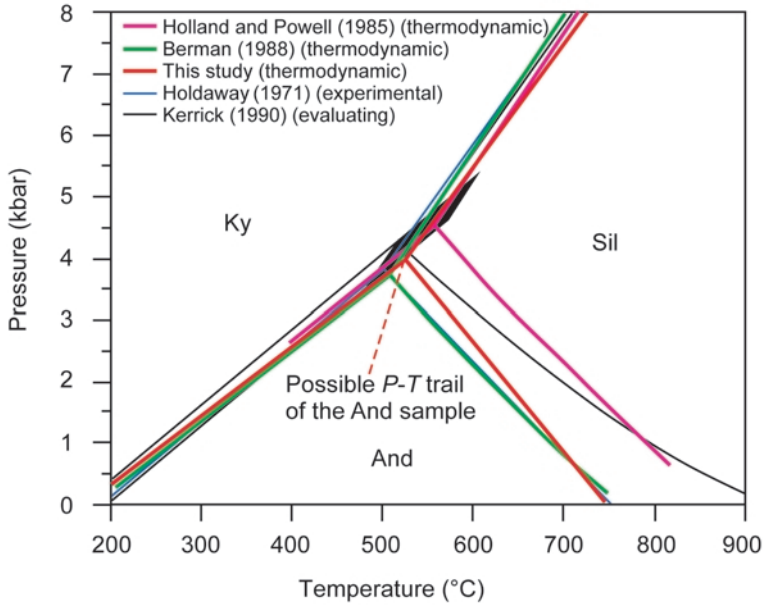

FIG. 7. Thermodynamically calculated phase relations of Ky, And and Sil. Data used in the calculation are from Burt *et al*. (2006), Liu *et al*. (2009, 2010), Robie and Hemingway (1995) and this study. The potential *P-T* trail experienced by the And material used in this study, as denoted by the thin broken curve, is estimated with the muscovite-biotite geothermometer of Hoisch (1989).

frequently cited experimental determination of Holdaway (1971) positioned the *P-T* condition of this invariant point at ~501ºC and 3.76 kbar (e.g. Whitney, 2002), and the most recent determination of Holdaway and Mukdhopadhyay (1993) positioned it at an almost identical *P-T* condition. As to the three univariant curves, Fig. 7 suggests that the *P-T* condition of the univariant curve of Ky + And or Ky + Sil appears well constrained whereas that of the univariant curve of And + Sil is still poorly resolved.

As mentioned previously, the And used in our study coexisted with muscovite, biotite, K-feldspar, quartz and ilmenite. The *P-T* trail of this material can be estimated with the muscovite-biotite geothermometer of Hoisch (1989), and the result is shown in Fig. 7. Clearly, this independent estimate corroborates the new thermodynamic calculation about the Ky-And-Sil system carried out in our study.

Acknowledgements

The authors thank Drs G.D. Gatta and M.D. Welch for their constructive comments which improved the paper. This investigation was supported financially by the Natural Science Foundation of China (Grant 40872033).

References

Beger, R.M. (1979) *Aluminum-silicon ordering in sillimanite and mullite*. PhD thesis, Harvard University, Massachusetts, USA, 312 pp.

Berman, R.G. (1988) Internally-consistent thermodynamic data for minerals in the system Na_2O-K_2O-CaO-MgO-FeO-Fe_2O_3-Al_2O_3-SiO_2-TiO_2-H_2O-CO_2. *Journal of Petrology*, **29**, 445–522.

Brace, W.F., Scholz, C.H. and La Mori, P.N. (1969) Isothermal compressibility of kyanite, andalusite, and sillimanite from synthetic aggregates. *Journal of Geophysical Research*, **74**, 2089–2098.

Burt, J.B., Ross, N.L., Angel, R.J. and Koch, M. (2006) Equations of state and structures of andalusite to 9.8 GPa and sillimanite to 8.5 GPa. *American Mineralogist*, **91**, 319–326.

Carpenter, M.A., Salje, E.K.H., Graeme-Barber, A., Wruck, B., Dove, M.T. and Knight, K.S. (1998) Calibration of excess thermodynamic properties and elastic constant variations associated with the $\alpha \rightleftharpoons \beta$ phase transition in quartz. *American Mineralogist*, **83**, 2–22.

Comodi, P., Zanazzi, P.F., Poli, S. and Schmidt M.W.

(1997) High-pressure behavior of kyanite: compressibility and structural deformations. *American Mineralogist*, **82**, 452–459.

Friedrich, A., Kunz, M., Winkler, B. and Le Bihan, T. (2004) High-pressure behavior of sillimanite and kyanite: compressibility, decomposition and indications of a new high-pressure phase. *Zeitschrift für Kristallogrphie*, **219**, 324–329.

Gatta, G.D., Nestola, F. and Walter, J.M. (2006) On the thermo-elastic behaviour of kyanite: a neutron powder diffraction study up to 1200ºC. *Mineralogical Magazine*, **70**, 309–317.

Hazen, R.M. and Finger, L.W. (1982) *Comparative Crystal Chemistry*. Wiley, New York.

Hoisch, T.D. (1989) A muscovite-biotite geothermometer. *American Mineralogist*, **74**, 565–572.

Holdaway, M.J. (1971) Stability of andalusite and the aluminum silicate phase diagram. *American Journal of Science*, **271**, 97–131.

Holdaway, M.J. and Mukdhopadhyay, B. (1993) A reevaluation of the stability relations of andalusite: thermochemical data and phase diagram for the alumino silicates. *American Mineralogist*, **78**, 298–315.

Holland, T.J.B. and Powell, R. (1985) An internally consistent thermodynamic dataset with uncertainties and correlations: 2. Data and results. *Journal of Metamorphic Geology*, **3**, 343–370.

Irifune, T., Kuroda, K., Minagawa, T. and Unemoto, M. (1995) Experimental study of the decomposition of kyanite at high pressure and high temperature. Pp. 35–44 in: *The Earth's Central Part: Its Structure and Dynamics* (T. Yukutake, editors). Terra Scientific publishing, Tokyo.

Kerrick, D.M. (1990) *The Al_2SiO_5 Polymorphs*. Reviews in Mineralogy, **22**. Mineralogical Society of American, Washington, D.C., 406 pp.

Liu, L. (1974) Disproportionation of kyanite to corundum plus stishovite at high pressure and high temperature. *Earth and Planetary Science Letters*, **24**, 224–228.

Liu, X., Nishiyama, N., Sanehira, T., Inoue, T., Higo, Y. and Sakamoto, S. (2006) Decomposition of kyanite and solubility of Al_2O_3 in stishovite at high pressure and high temperature conditions. *Physics and Chemistry of Minerals*, **33**, 711–721.

Liu, X., Shieh, S.R., Fleet, M.E. and Zhang, L. (2009) Compressibility of a natural kyanite to 17.5 GPa. *Progress in Natural Science*, **19**, 1281–1286.

Liu, X., He, Q., Wang, H., Fleet, M.E. and Hu, X. (2010) Thermal expansion of kyanite at ambient pressure: an X-ray powder diffraction study up to 1000ºC. *Geoscience Frontiers*, **1**, 91–97.

Matsui, M. (1996) Molecular dynamics study of the structures and moduli of crystals in the system CaO-MgO-Al_2O_3-SiO_2. *Physics and Chemistry of Minerals*, **23**, 345–353.

Oganov, A.R. and Brodholt, J.P. (2000) High-pressure phases in the Al_2SiO_5 system and the problem of aluminous phase in the Earth's lower mantle: ab initio calculations. *Physics and Chemistry of Minerals*, **27**, 430–439.

Ono, S., Nakajima, Y. and Funakoshi, K. (2007) In situ observation of the decomposition of kyanite at high pressures and high temperatures. *American Mineralogist*, **92**, 1624–1629.

Ralph, R.L., Finger, L.W., Hazen, R.M. and Ghose, S. (1984) Compressibility and crystal structure of andalusite at high pressure. *American Mineralogist*, **69**, 513–519.

Ren, L., Geng, Y., Wang, Y. and Zhao, Y. (2007) On the protolith of the sillimanite gneisses in the Larsemann Hills, East Antarctica. *Earth Science Frontiers*, **14**, 75–84.

Ren, L., Yang, C., Wang, Y., Liu, X. and Zhao, Y. (2009) Formation of sillimanite in the high-grade quartzofeldspathic gneisses and its relations with deformation-metamorphism-anatexis: a case study in the Larsemann Hills, East Antarctica. *Acta Petrologica Sinica*, **25**, 1937–1946.

Robie, R.A. and Hemingway, B.S. (1995) Thermodynamic properties of minerals and related substances at 298.15 K and 1 bar (10^5 pascals) pressure and at high temperatures. *US Geological Survey Bulletin*, **2131**, 461 pp.

Schmidt, M.W., Poli, S., Comodi, P. and Zanazzi, P.F. (1997) High-pressure behavior of kyanite: decomposition of kyanite into stishovite and corundum. *American Mineralogist*, **82**, 460–466.

Skinner, B.J., Clark, S.P. and Appleman, D.E. (1961) Molar volumes and thermal expansions of andalusite, kyanite, and sillimanite. *American Journal of Science*, **259**, 651–668.

Todd, S.S. (1950) Heat capacities at low temperatures and entropies at 298.16 K of andalusite, kyanite, and sillimanite. *Journal of the American Chemical Society*, **72**, 4742–4743.

Vaughan, M.T. and Weidner, D.J. (1978) The relationship of elasticity and crystal structure in andalusite and sillimanite. *Physics and Chemistry of Minerals*, **3**, 133–144.

Whitney, D.L. (2002) Coexisting andalusite, kyanite, and sillimanite: sequential formation of three Al_2SiO_5 polymorphs during progressive metamorphism near the triple point, Sivrihisar, Turkey. *American Mineralogist*, **87**, 405–416.

Winkler, B., Hytha, M., Warren, M.C., Milman, V., Gale, J.D. and Schreuer, J. (2001) Calculation of the elastic constants of the Al_2SiO_5 polymorphs andalusite, sillimanite and kyanite. *Zeitschrift für Kristallogrphie*, **216**, 67–70.

Winter, J.K. and Ghose, S. (1979) Thermal expansion

and high-temperature crystal chemistry of the Al_2SiO_5 polymorphs. *American Mineralogist*, **64**, 573–586.

Yang, H., Downs, R.T., Finger, L.W., Hazen, R.M. and Prewitt, C.T. (1997*a*) Compressibility and crystal structure of kyanite, Al_2SiO_5, at high pressure. *American Mineralogist*, **82**, 467–474.

Yang, H., Hazen, R.M., Finger, L.W., Prewitt, C.T. and Downs, R.T. (1997*b*) Compressibility and crystal structure of sillimanite, Al_2SiO_5, at high pressure. *Physics and Chemistry of Minerals*, **25**, 39–47.

Zhou, S. and Feng, Z. (1999) Mineralogical characteristics and usage of macrocrystal andalusite from Xixia, Henan. *Mineral Resources and Geology*, **13**, 40–43.